Preprint of: Ciupak, O., Demkowicz, S., Rachoń, J., Biernacki, K., Czubak, P., Martyna, A., Masłyk, M., Datta, M., Rak, J., & Daśko, M. (2025). Novel nonsteroidal steroid sulfatase inhibitors containing glutamic acid unit. EUROPEAN JOURNAL OF MEDICINAL CHEMISTRY, 291, 117627. https://doi.org/10.1016/j.ejmech.2025.117627

Novel nonsteroidal steroid sulfatase inhibitors containing glutamic acid unit

Olga Ciupak *[a], Sebastian Demkowicz [a], Janusz Rachon [a], Karol Biernacki [a], Paweł Czubak [b], Aleksandra Martyna [b], Maciej Masłyk [b], Konrad Kubiński [b], Magdalena Datta [c], Janusz Rak [c], and Mateusz Daśko **[d]

[a] Department of Organic Chemistry, Faculty of Chemistry, Gdansk University of Technology, Narutowicza 11/12, 80-233 Gdansk, Poland.
[b] Department of Molecular Biology, Faculty of Medicine, The John Paul II Catholic University of Lublin, Konstantynów 1i, 20-708 Lublin, Poland.
[c] Laboratory of Biological Sensitizers, Department of Physical Chemistry, Faculty of Chemistry, University of Gdańsk, Wita Stwosza 63, 80-308 Gdańsk, Poland.
[d] Department of Inorganic Chemistry, Faculty of Chemistry, Gdansk University of Technology, Narutowicza 11/12, 80-233 Gdansk, Poland.

Corresponding authors: ** Mateusz Daśko (e-mail: mateusz.dasko@pg.edu.pl), * Olga Ciupak (e-mail: olga.ciupak@pg.edu.pl).

Keywords: cancer, steroid sulfatase, STS inhibitors, triazole, molecular docking.

Abstract
In the present work, we designed and successfully synthesized novel steroid sulfatase (STS) inhibitors based on coumarin, tyramine, triazole, and flavone cores with an additional glutamic acid residue in the structure. The molecular modeling studies revealed that designed derivatives have potential to bind to the molecular target active site, at least theoretically. The biological activity of synthesized compounds was evaluated under a two-step procedure including enzymatic assay and cellular studies using human choriocarcinoma JEG-3 cells. Among the synthesized compounds, the derivative **VK** was the most active in both enzymatic and cellular experiments. This result agreed with the molecular modeling data, which indicated that derivative **VK** demonstrates the highest affinity to the STS active site. In the enzymatic assay, the remaining STS activity values of 12.97, 17.58, and 20.52% were observed at 10, 1, and 0.1 μM concentrations of compound **VK**, respectively. The IC_{50} value of 22 nM determined in an experiment with JEG-3 cells for compound **VK** was close to the IC_{50} value determined for the reference STS inhibitor *Irosustat* (2.7 nM), indicating that **VK** is a very promising candidate for further preclinical investigations.

Introduction
The role of hormones in cancer is further complicated by various signaling pathways that interact with hormonal signals. For instance, the estrogen receptor (ER) signaling pathway regulates gene expression related to cell proliferation and survival, thereby influencing the aggressiveness of tumors [1]. Additionally, the crosstalk between DNA damage response mechanisms and hormone signaling pathways underscores the multifaceted nature of hormonal influence on cancer biology [2]. Moreover, the bioconversion of hormones, mainly through the action of steroid sulfatase (STS), plays a significant role in the growth and progression of hormone-dependent cancers, such as breast and prostate cancer. STS catalyzes the hydrolysis of inactive steroid sulfates into their active forms, thereby facilitating the local production of estrogens like estradiol, crucial for tumor growth in hormone-responsive tissues [3]. This process is particularly relevant in postmenopausal women, where the extragonadal synthesis of estrogens from sulfated precursors becomes the primary source of estrogens, contributing to the pathogenesis of hormone-dependent types of carcinoma [4].

Research indicates that elevated STS levels is associated with increased tumor proliferation in estrogen receptor-positive breast cancer [5]. Inhibition of STS has emerged as a therapeutic strategy, with compounds like *Irosustat* **1** (**Figure 1**) demonstrating efficacy in clinical trials by effectively reducing tumor cell proliferation and altering local estrogen levels [6]. In the last few decades, scientists have made intensive efforts in finding novel and effective steroidal and non-steroidal STS inhibitors. However, the clinical usage of STS inhibitors based on a steroid core has, in some cases, proven problematic due to the observed side effects, including the estrogenic properties of their metabolites which stimulated tumor growth. Therefore, the synthesis of non-steroidal STS inhibitors based on different scaffolds became a priority in the development of drug candidates with greater clinical applications [3].

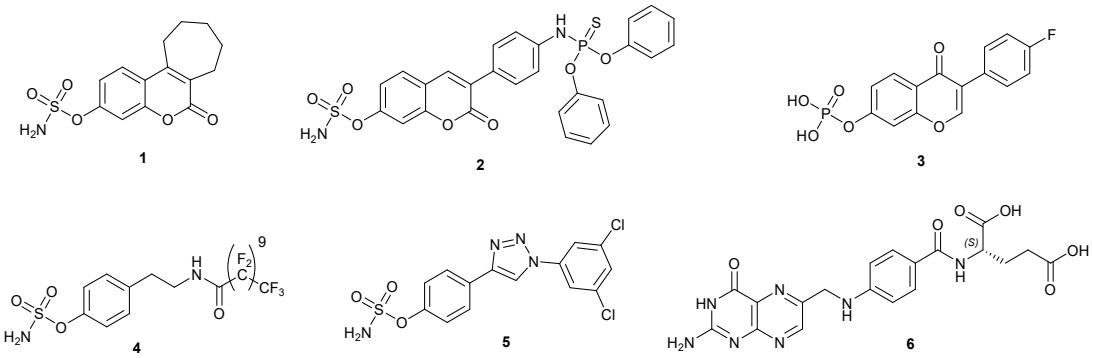

Figure 1. Chemical structures of non-steroidal STS inhibitors **1-5** and FA **6**.

Coumarin, present in the chemical structure of *Irosustat* **1**, has proven to be an excellent example of a non-steroidal core that enables effective binding to the STS active site. To date, many coumarin-based STS inhibitors have been developed, including derivatives synthesized in our research group, *e.g.*, compound **2** [7]. Furthermore, we have successfully applied other non-steroidal motifs in the structures of STS inhibitors including flavones (*e.g.*, compound **3**) [8], tyramines (*e.g.*, compound **4**) [9], and triazoles (*e.g.*, compound **5**) [10], synthesizing agents that demonstrate high STS inhibitory potency.

In the present study, we designed and successfully synthesized a series of novel STS inhibitors based on the aforementioned non-steroidal cores. Importantly, we modified their structure by introducing an additional glutamic acid residue in the structure. The addition of glutamic acid, an amino acid that plays a critical role in various physiological processes, to the chemical structure of biologically active agents has been shown to significantly influence their biological activities and therapeutic properties [11]. For example, an addition of a glutamic acid unit can significantly enhance the solubility of compounds, thereby improving their efficacy in clinical applications [12, 13]. Moreover, by adding glutamic acid residue we hoped that our non-steroidal STS inhibitors would exhibit structural similarities to folic acid (FA) **6**, in which the glutamic acid is present, thus enabling their transport to cancer cells in a similar manner. The folate uptake in tissues relies on the diverse transport systems including folate receptors (FRs), which occurs with high-affinity and selectivity. The FRs expression is observed mainly in tissues important for the embryonic development process and kidney [14]. While the level of FRα, the most widely expressed among the three FR isoforms, in normal tissues is very low it is observed that the FRα expression levels are high in numerous types of cancers [15]. The higher expression of FRα is associated with an increased demand from rapidly dividing cancer cells. Therefore, the folate dependency of tumors has been therapeutically applied and FRα has been considered as a promising molecular target for cancer treatment strategies [16].

Results and discussion

Molecular docking

As the first step of our investigation, the molecular docking studies were carried out to theoretically evaluate 1) the effect of introducing a glutamic acid residue into the structure of non-steroidal STS inhibitors on the binding efficiency to the STS active site, and 2) the manner and binding potency of the designed derivatives to the FRα binding site and to verify whether they could potentially be transported into the cancer cell by receptors involved in the folate uptake mechanism. Crystal structures of both proteins were collected from the Protein Data Bank (PDB) (STS: 1P49 and FRα: 4LRH), which were properly prepared before the docking calculations. The docking procedure for the optimized ligands was carried out using AutoDock Vina 1.1.2 software (Molecular Graphics Laboratory, The Scripps Research Institute, La Jolla, CA).

Initially, we designed the structures for the first series of novel non-steroidal STS inhibitors based on coumarin, triazole, flavone, and tyramine cores with the glutamic acid unit existing as either a free carboxylic acid or a methyl ester. In the case of docking to STS, the calculated free energy of binding values for the proposed structures of potential STS inhibitors **I-IVA-B** were at a satisfactory level ranging from -4.8 to -7.0 kcal/mol for STS (**Table 1**). Importantly, in most cases, the free energy of binding values for the designed compounds were comparable to, or slightly lower than, those for the reference *Irosustat* **1** (-6.3 kcal/mol) suggesting that the introduction of the glutamic acid residue should not decrease STS inhibitory activity of the compounds. According to the collected data, the derivatives based on coumarin **IIB** and flavone **IVB** cores demonstrated the highest affinity to the STS active site, with a free energy of binding value of -7.0 kcal/mol in both cases. On the other hand, the free energies of binding calculated for compounds **I-IVA-B** in the experiment with FRα occurred to be low in a range of -7.9 to -9.5 kcal/mol. Even though in all cases the values of free energy of binding were slightly higher compared to FA (-10.5 kcal/mol), the molecular docking studies showed that the designed compounds are well accommodated in the protein's binding site and they may potentially be transported into the cancer cell by FRα.

Table 1. Results of molecular docking analysis for compounds **I-IVA-B**, *Irosustat* **1**, and FA, obtained using Auto Dock Vina 1.1.2 software.

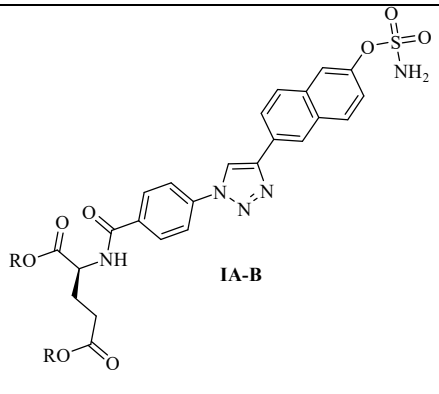

IA-B

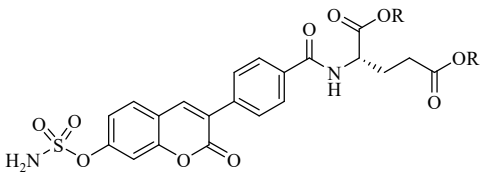

IIA-B

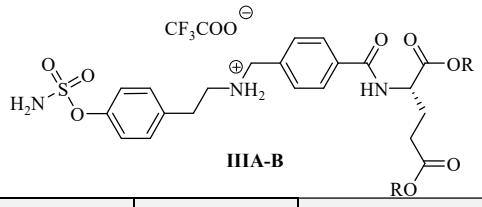

IIIA-B

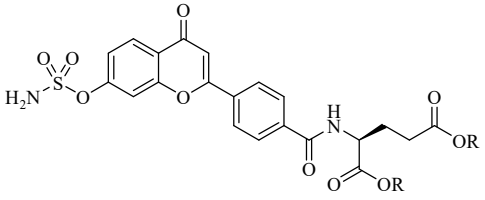

IVA-B

No.	R	Free energy of binding [kcal/mol]

		STS	FRα
IA	Me	-6.0	-8.4
IB	H	-6.9	-8.4
IIA	Me	-6.2	-9.1
IIB	H	-7.0	-7.9
IIIA	Me	-6.6	-8.0
IIIB	H	-6.4	-9.5
IVA	Me	-4.8	-9.3
IVB	H	-7.0	-9.0
Irosustat **1**	-	-6.3	-
FA **6**	-	-	-10.5

In addition, the identification of potential interactions in the resulting complexes of designed compounds **I-IVA-B** and STS and FRα was carried out using BIOVIA, Dassault Systèmes, Discovery Studio Visualizer. The detailed data are summarized in **Table S1** and **Table S2**, *Supporting information*. The obtained results proved that compounds **I-IVA-B** are theoretically capable of forming several strong interactions with both examined proteins. In the case of STS-ligand complexes, these include π-alkyl, π-sulfur, π-sigma, hydrogen, or hydrogen-carbon interactions. In the case of complexes with FRα, a greater number of different interactions were identified, that were not detected in the case of complexes with STS, including π-π (staggered stacking and T-shaped) and π-cation interactions. None of the proposed compounds demonstrated significantly more favorable interactions with STS and FRα compared to other derivatives of the series. However, the number of identified interactions indicated that the designed compounds may exhibit promising binding abilities to the active sites of both proteins. Furthermore, the molecular docking studies proved that the sulfamate pharmacophores of all designed compounds are within a short distance from the fGly75 residue of STS, which is crucial for the enzymatic reaction. The distance between the sulfur atom of the sulfamate group of the representative compound **IB** and the oxygen atom of fGly75 was 2.81 Å, while for the reference compound, it was 3.16 Å (**Figure 2**). This may indicate a high probability of STS inhibition according to the mechanism proposed in recent literature [6].

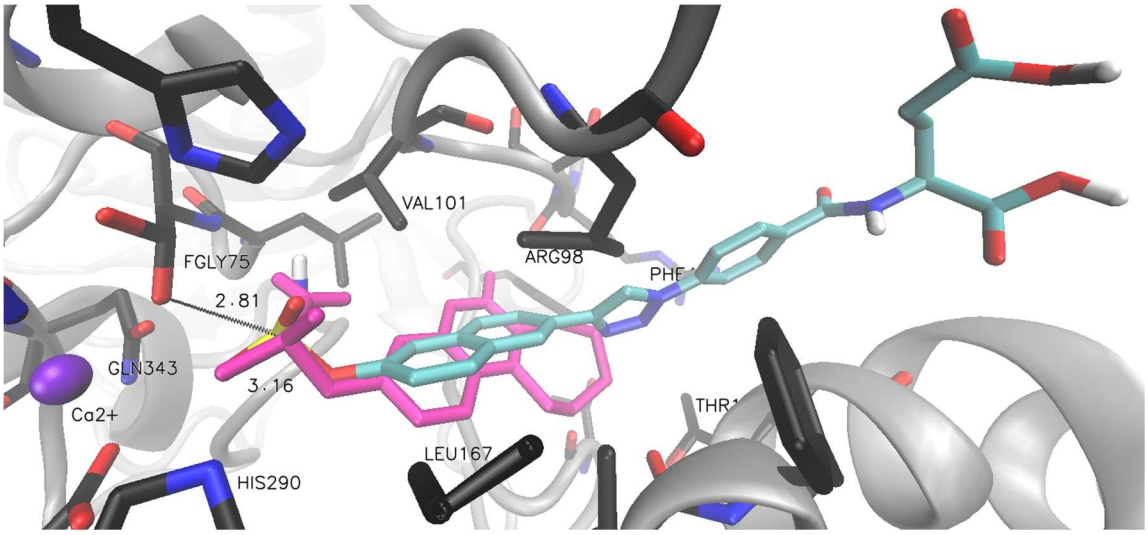

Figure 2. Predicted binding mode of compound **IB** (CPK coloured) and *Irosustat* **1** (pink) in the STS active site with distances to fGly75 (Å).

The docking calculations were repeated for the next series of potential STS inhibitors based on a triazole-containing core, which was selected as the most favorable for STS inhibitory potency (see further details in the *Biological Evaluation* section). In the second series of compounds **VA-L**, we modified the structure of parent derivatives **IA** and **IB** by adding a fluorine atom in the *meta* position of the terminal phenyl ring relative to the triazole unit. We hypothesized that this modification would enhance the STS inhibitory potency due to the creation of plausible interactions between the halogen atom and amino acid residues in the active site of STS as observed in the other series of STS inhibitors based on triazole core [10, 17, 18]. Moreover, the influence of the glutamic acid residue position in the terminal phenyl ring, as well as a type of the ester group on STS inhibitory activity was evaluated. The results for the second series of compounds **VA-L** are summarized in **Table 2**.

Table 2. Results of molecular docking analysis for compounds **VA-L**, *Irosustat* **1**, and FA, obtained using Auto Dock Vina 1.1.2 software.

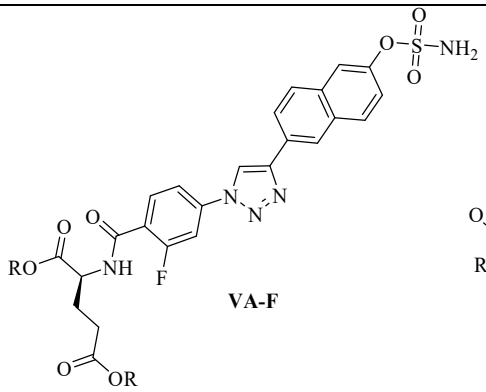

VA-F

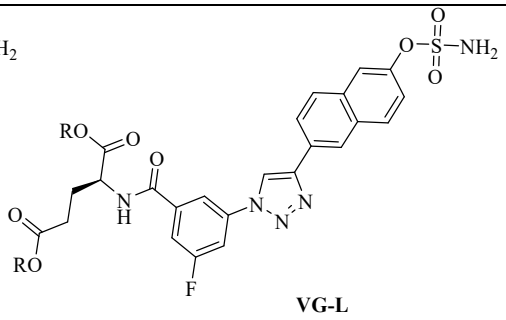

VG-L

No.	R	Free energy of binding [kcal/mol]	
		STS	FRα
VA	Me	-6.5	-10.4
VB	Et	-7.4	-9.0
VC	^{i}Pr	-7.6	-9.5
VD	^{t}Bu	-4.1	-9.5
VE	Bn	-7.1	-9.0
VF	H	-7.5	-11.0
VG	Me	-6.9	-10.3
VH	Et	-7.5	-9.8
VI	^{i}Pr	-6.4	-9.0
VJ	^{t}Bu	-7.8	-9.8
VK	Bn	-9.7	-9.8
VL	H	-7.8	-10.9
Irosustat **1**	-	-6.3	-
FA **6**	-	-	-10.5

In general, for both proteins the values of free energy of binding calculated for potential STS inhibitors of the second series were significantly lower than those calculated for the first series of compounds indicating that they may demonstrate higher affinity to the active sites of STS and FRα. Regarding the experiment with STS as a molecular target, in most cases, derivatives with a glutamic acid residue at *meta* position of the terminal phenyl ring

relative to the triazole ring, demonstrated lower binding energy values than their 4-substituted analogs, *e.g.*, derivative **VK** with the lowest value of free energy of binding (-9.7 kcal/mol) among all compounds of the series. On the other hand, in the case of docking to FRα, no significant differences were observed in the binding potency between 3- or 4- substituted analogs. The lowest free energy of binding were calculated for derivatives **VF** and **VL** (-11.0 and -10.9 kcal/mol, respectively) indicating that free carboxylic acid groups may be favorable in binding with FRα. Importantly, these two analogs **VF** and **VL** demonstrated slightly lower free energy of binding than native ligand FA (-10.5 kcal/mol) proving high binding abilities.

The identification of potential interactions in the resulting complexes of designed compounds of the second series **VA-L** using BIOVIA software was carried out. In the case of ligand-STS complexes, similarly to the first series of STS inhibitors, many possible interactions were detected, such as hydrogen bonding, hydrogen-carbon bonding, π-sulfur, π-alkyl, metal-acceptor, π-π or π-cation (**Table S3**, *Supporting information*). Importantly, in this series of compounds additional interactions based on halogen bonding were detected indicating that the presence of fluorine atom may be beneficial for binding to STS. Furthermore, the interactions based on halogen bonding were also detected in the case of ligand-FRα complexes. Such additional interactions may be responsible for lower energy of binding values calculated for compounds of second series **VA-L** and may influence their higher affinity to FRα. All detected interactions between compounds **VA-L** and FRα are listed in **Table S4**, *Supporting information*. Furthermore, the distance between the sulfur atoms of the compounds **VA-L** and the oxygen atom of the fGly75 residue of STS was also measured. As shown in **Figure 3** for representative compound **VK** the distance was 3.02 Å and comparable with *Irosustat* **1** (3.16 Å), which suggests that the inhibition by the sulfamate group transfer may take place.

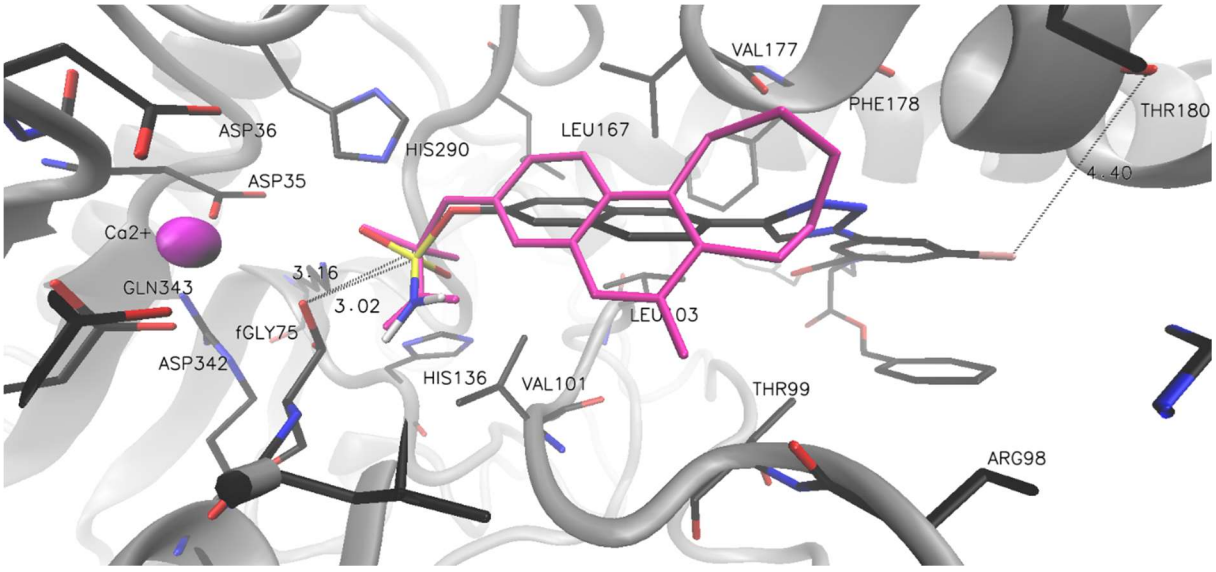

Figure 3. Predicted binding mode of compound **VK** (black) and *Irosustat* **1** (pink) in the STS active site with distances to fGly75 (Å).

Synthesis

The newly designed compounds **IA-B**, 1,2,3-triazole derivatives, were synthesized according to the route shown in **Scheme 1**. The first step of the synthesis involved the preparation of 6-((trimethylsilyl)ethynyl)naphthalen-2-ol **7** by the Sonogashira coupling reaction between 6-bromo-2-naphthol and trimethylsilylacetylene. The next step included the preparation of methyl 4-aminobenzoate **8** using the classical esterification reaction with *para*-aminobenzoic

acid, thionyl chloride, and methanol. Subsequently, a 1,3-dipolar cycloaddition reaction was carried out using azide (obtained from compound **8** by the reaction with *tert*-butyl nitrite (*t*-BuONO) and trimethylsilyl azide ($TMSN_3$)) and **7** in the presence of copper(II) sulfate pentahydrate, 1M aqueous solution of sodium ascorbate solution and 1M tetra-*n*-butylammonium fluoride (TBAF) solution in tetrahydrofuran (THF). Then, the obtained compound **9** was treated with an aqueous solution of lithium hydroxide leading to the formation of derivatives **10**. In the next step the obtained compound **10** and glutamic acid dimethyl ester hydrochloride were coupled using 1-hydroxybenzotriazole (HOBt) and 2-(1*H*-benzotriazole-1-yl)-1,1,3,3-tetramethylaminium tetrafluoroborate (TBTU) as coupling reagents in the presence of *N*,*N*-diisopropylethylamine (DIPEA) resulting in the formation of compound **11**. Next, compound **11** was used in two different reactions. In the first, the methyl esters were hydrolyzed using an aqueous solution of lithium hydroxide, yielding compound **12**. Finally, compounds **11** and **12** dissolved in *N*,*N*-dimethylacetamide (*N*,*N*-DMA) were treated with commercially available sulfamoyl chloride, that was dissolved in acetonitrile (ACN). After the standard isolation protocol, the desired derivatives **IA-B** were obtained.

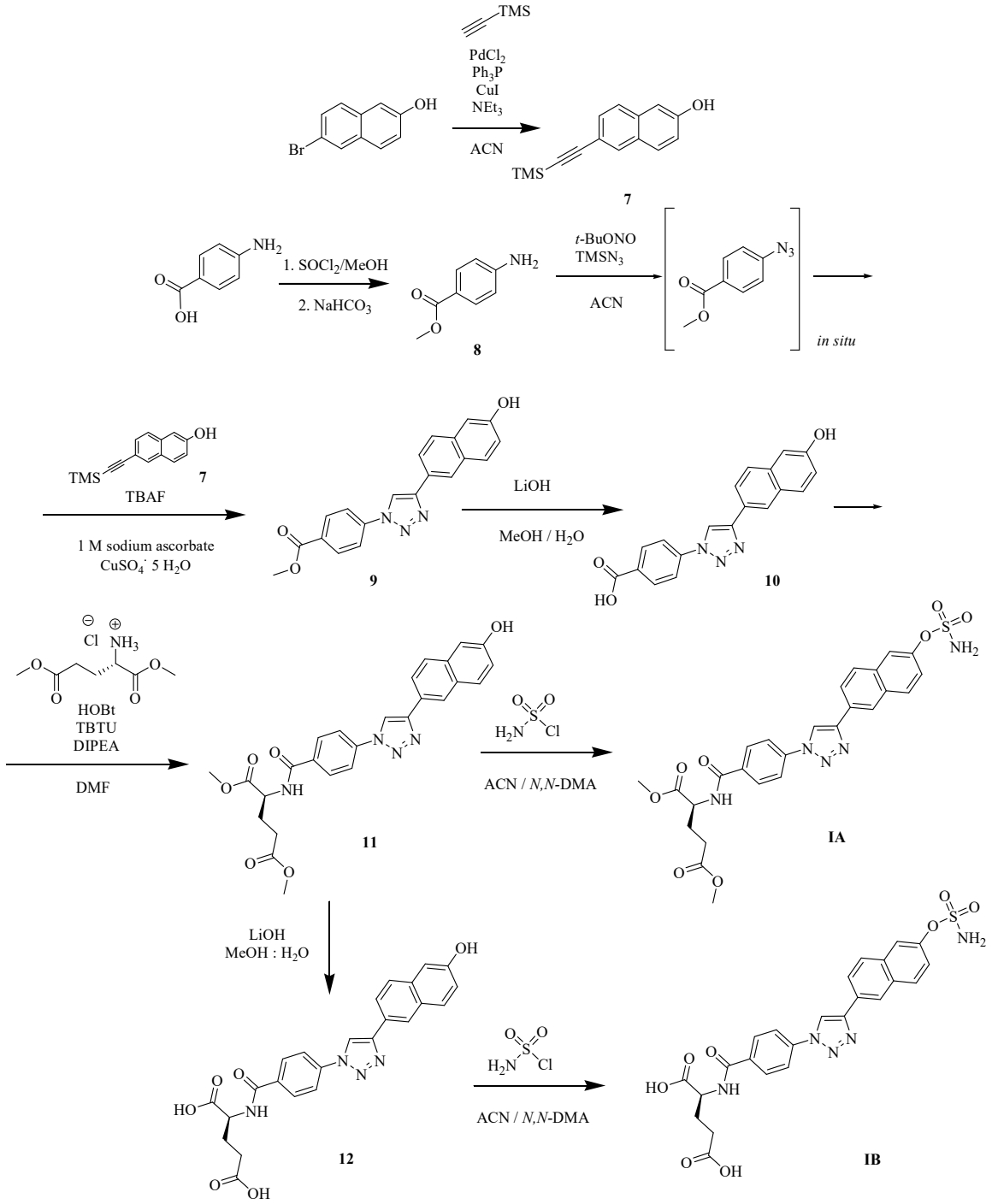

Scheme 1. Synthetic pathway for compounds **IA** and **IB**.

The compounds **IIA-B** based on coumarin derivatives were synthesized according to the route shown in **Scheme 2**. The first step of the synthesis involved the preparation of methyl 4-(2-methoxy-2-oxoethyl)benzoate **13** by the esterification using 4-(carboxymethyl)benzoic acid, thionyl chloride, and methanol. In the next step, the selective hydrolysis of one methyl ester group with 1.1 eq K_2CO_3 was performed. Subsequently, intermediate **14** was transformed *in situ* to acid chloride using $SOCl_2$, which was then treated with 2,4-dihydroxyaldehyde in the presence of K_2CO_3 to yield derivative **15**. Then, the hydrolysis of the methyl ester group using an aqueous solution of lithium hydroxide led to compound **16**, which was coupled with corresponding glutamic acid hydrochloride ester using

HOBt and TBTU as coupling reagents in the presence of DIPEA resulting in the formation of compounds **17** and **18**. Next, compounds **17** and **18** were sulfamoylated using a previously prepared sulfamoyl chloride solution in ACN. After standard isolation protocol, the desired derivatives **IIA** and **19** were obtained. In the end, compound **19** was converted to the final compound **IIB** by treatment with trifluoroacetic acid (TFA).

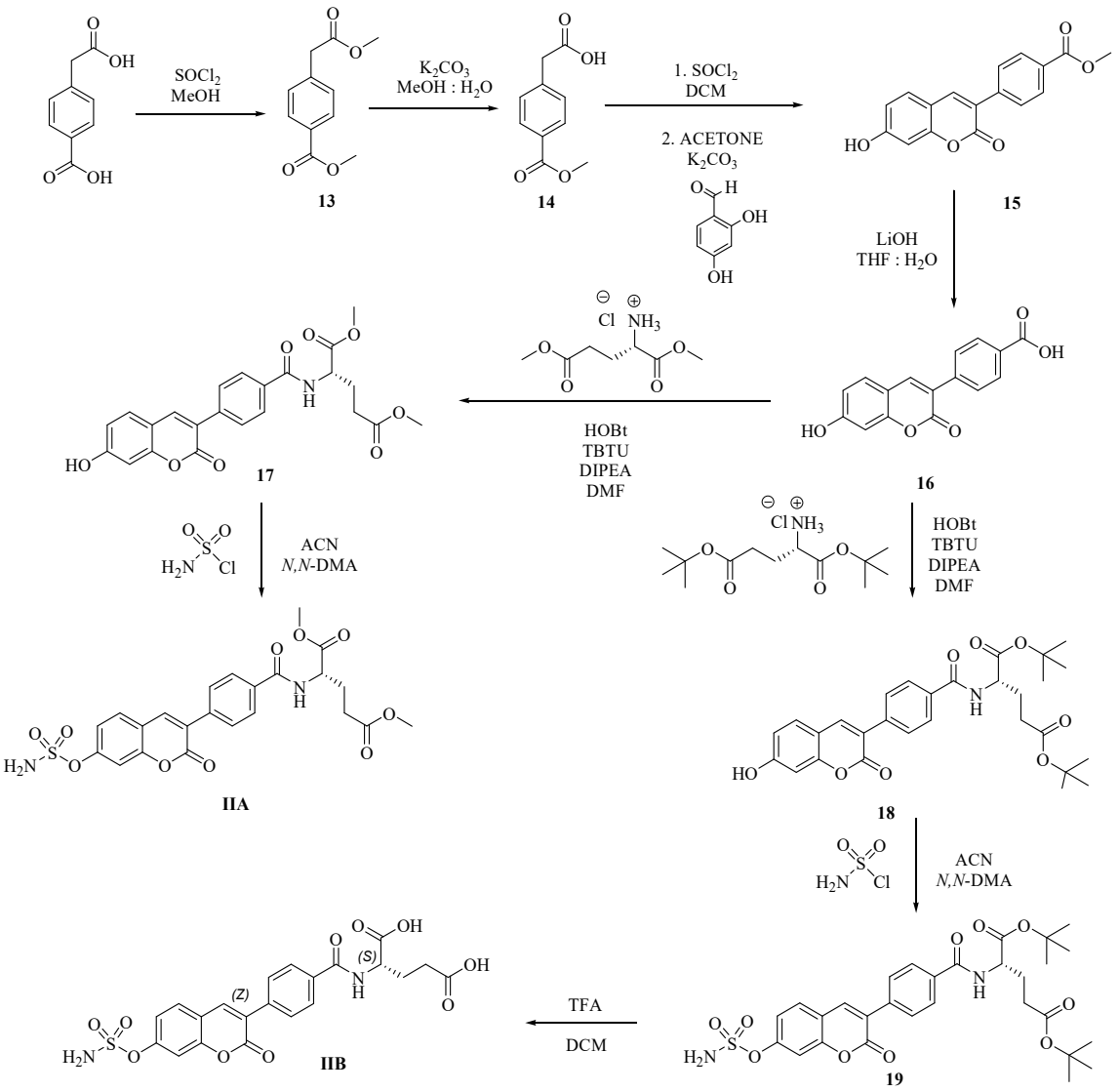

Scheme 2. Synthetic pathway for compounds **IIA** and **IIB**.

The newly designed tyramine derivatives **IIIA-B** were synthesized according to the route shown in **Scheme 3**. The first step of the synthesis involved the preparation of 4-(((4-hydroxyphenethyl)amino)methyl)benzoic acid **20** by a reductive amination reaction between 4-(2-aminoethyl)phenol and 4-formylbenzoic acid and $NaBH_3CN$. Next, the amine group of compound **20** was protected by a *tert*-butoxycarbonyl (BOC) group using di-*tert*-butyl dicarbonate (Boc_2O). Then, coupling reactions of the obtained compound **21** and corresponding glutamic acid hydrochloride ester using HOBt and TBTU as coupling reagents in the presence of DIPEA led to the formation of compounds **22** and **23**. Next, the obtained compounds **22** and **23** were sulfamoylated using a previously prepared sulfamoyl chloride solution in ACN. Finally, BOC protected derivatives **24** and **25** were transformed into the final compounds **IIIA** and **IIIB** by the treatment with TFA.

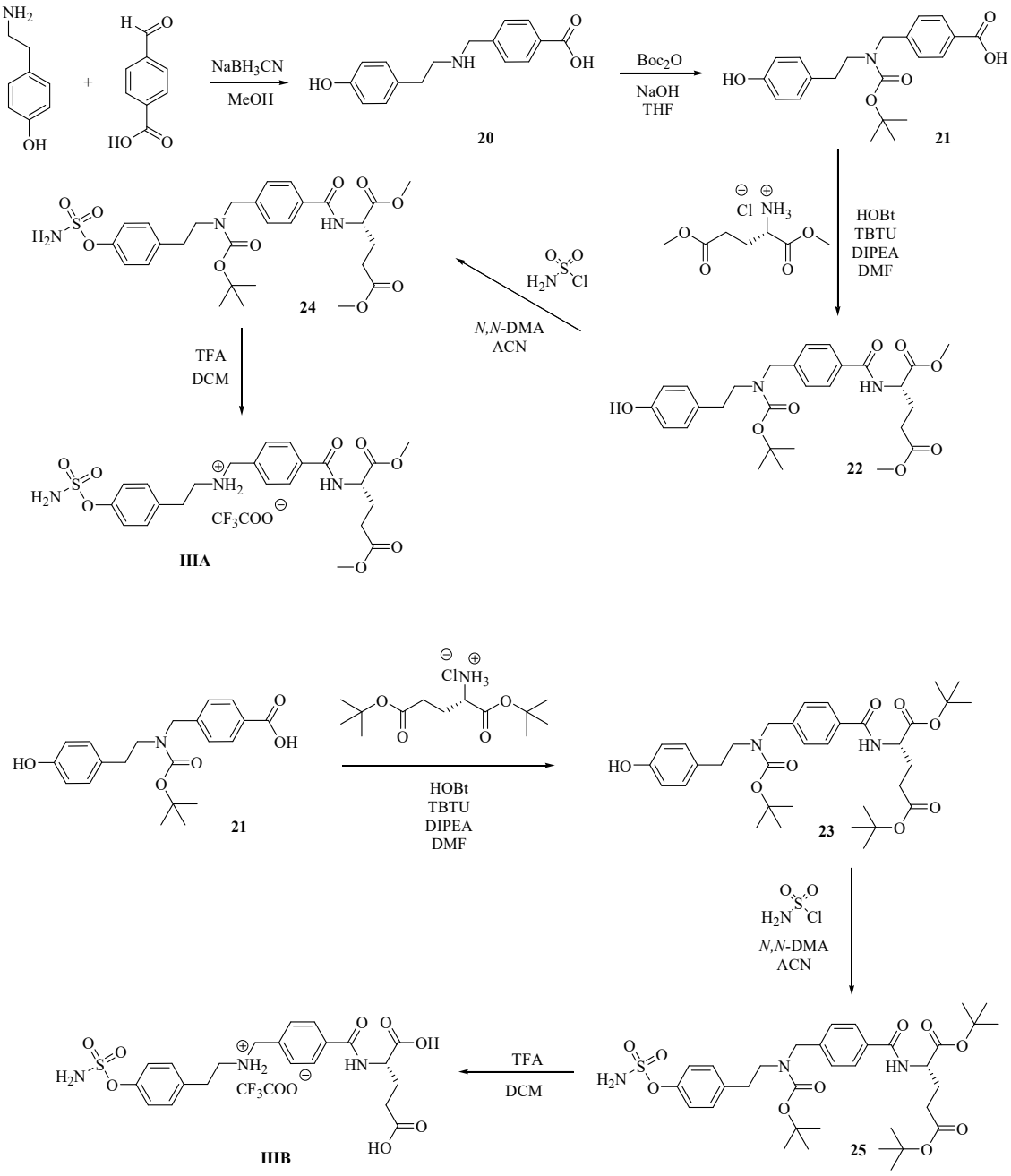

Scheme 3. Synthetic pathway for compounds **IIIA** and **IIIB**.

The flavone derivatives **IVA-B** were synthesized according to the route shown in **Scheme 4**. The first step of the synthesis involved the preparation of compound **26** according to the synthetic protocol described by Kobzar, O.L., *et al.* [19]. Next, compound **26** was treated with pyridine hydrochloride (PY•HCl) to remove the methyl group. The obtained derivative **27** was coupled with dimethyl and di-*tert*-butyl derivatives of glutamic acid to give compounds **28** and **29**. Then, compounds **28** and **29** were treated with sulfamoyl chloride solution in ACN to give compounds **IVA** and **30**. Finally, derivative **30** containing a BOC protective group was transformed into the final compound **IVB** in a reaction with TFA.

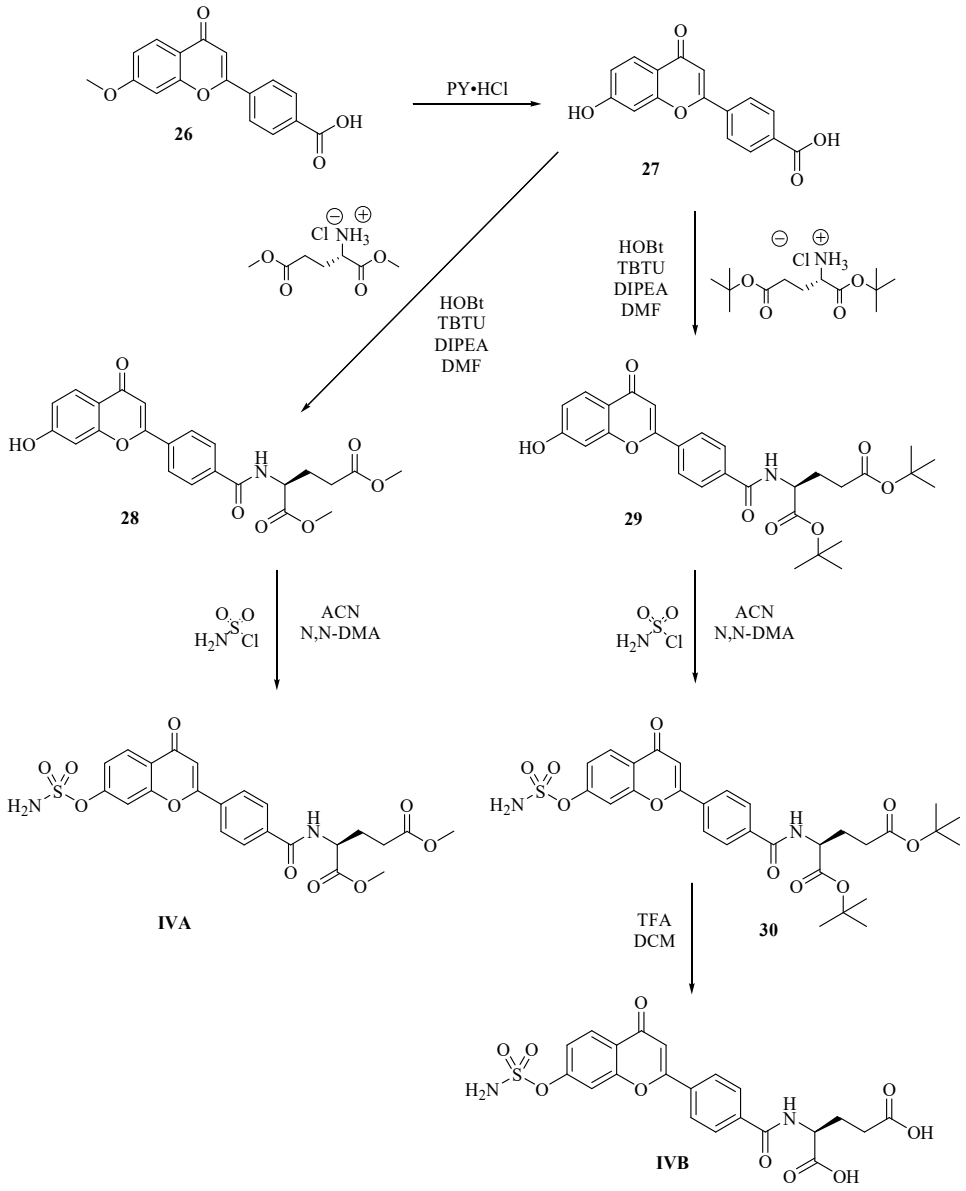

Scheme 4. Synthetic pathway for compounds **IVA** and **IVB**.

After the initial biological evaluation of inhibitors **I-IVA-B**, it was decided that the second series of STS inhibitors based on triazole core would be designed and synthesized. In the second series of compounds, an additional fluorine atom in *meta* position of the terminal phenyl ring, relative to the triazole unit, was introduced. Additionally, we synthesized derivatives, in which the structure of the glutamic acid residue was also moved to second *meta* position relative to the triazole ring. Furthermore, different alcohols were utilized in the creation of the ester groups of glutamic acid. The first part of compounds with the glutamic acid residue introduced in *para* position relative to triazole ring, were synthesized according to the route shown in **Scheme 5**. The first step of the synthesis involved the preparation of compound **31** using the esterification reaction with 4-amino-2-fluorobenzoic acid, thionyl chloride, and methanol. In the next step, a 1,3-dipolar cycloaddition reaction was carried out using the azide derivative **32** (obtained *in situ* from compound **31**) and **7** in the presence of $CuSO_4 \bullet 5\,H_2O$, sodium ascorbate, and TBAF. Then, the hydrolysis of the obtained compound **33** was carried out using lithium hydroxide solution. The hydroxyl group of compound **34** was protected with *tert*-butyldimethylsilyl (TBDMS) group. The next step of the synthesis

included a series of coupling reactions between derivative **35** and the corresponding glutamic acid esters using HOBt and TBTU as coupling reagents in the presence of DIPEA yielding compounds **36A-E**. Next, obtained compounds **36A-E** were treated with TBAF in THF to deprotect hydroxyl groups, which were finally transformed into sulfamate moiety in compounds **VA-E** using sulfamoyl chloride solution in ACN. Compound **VF** was obtained from derivative **VD**, which was treated with a solution of TFA in dichloromethane (DCM). The second part of compounds with the glutamic acid residue introduced in *meta* position were synthesized analogously using 3-amino-5-fluorobenzoic acid as a starting material (**Scheme 6**).

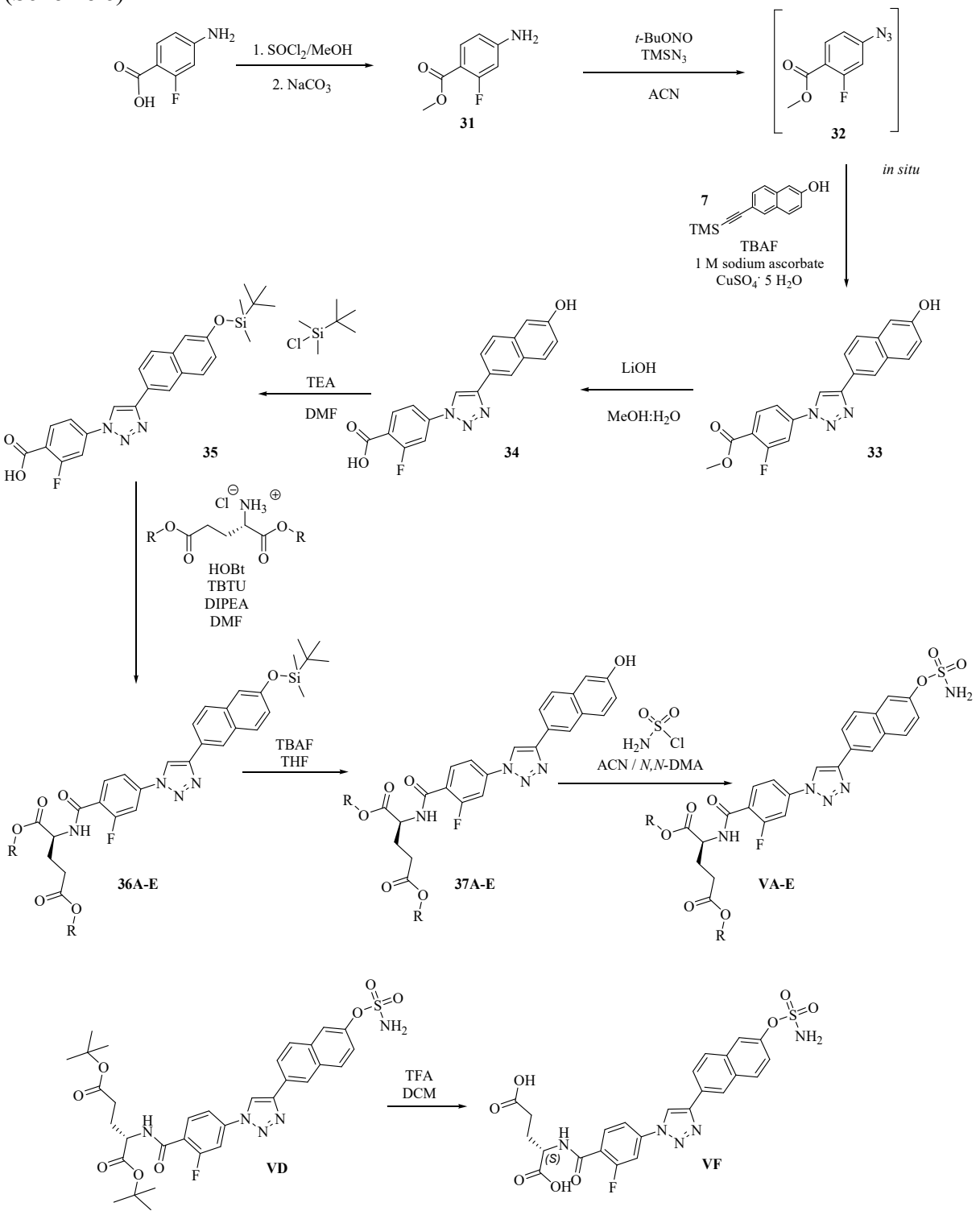

Scheme 5. Synthetic pathway for compounds **VA-F** (R = Me, Et, ^{i}Pr, ^{t}Bu, Bn).

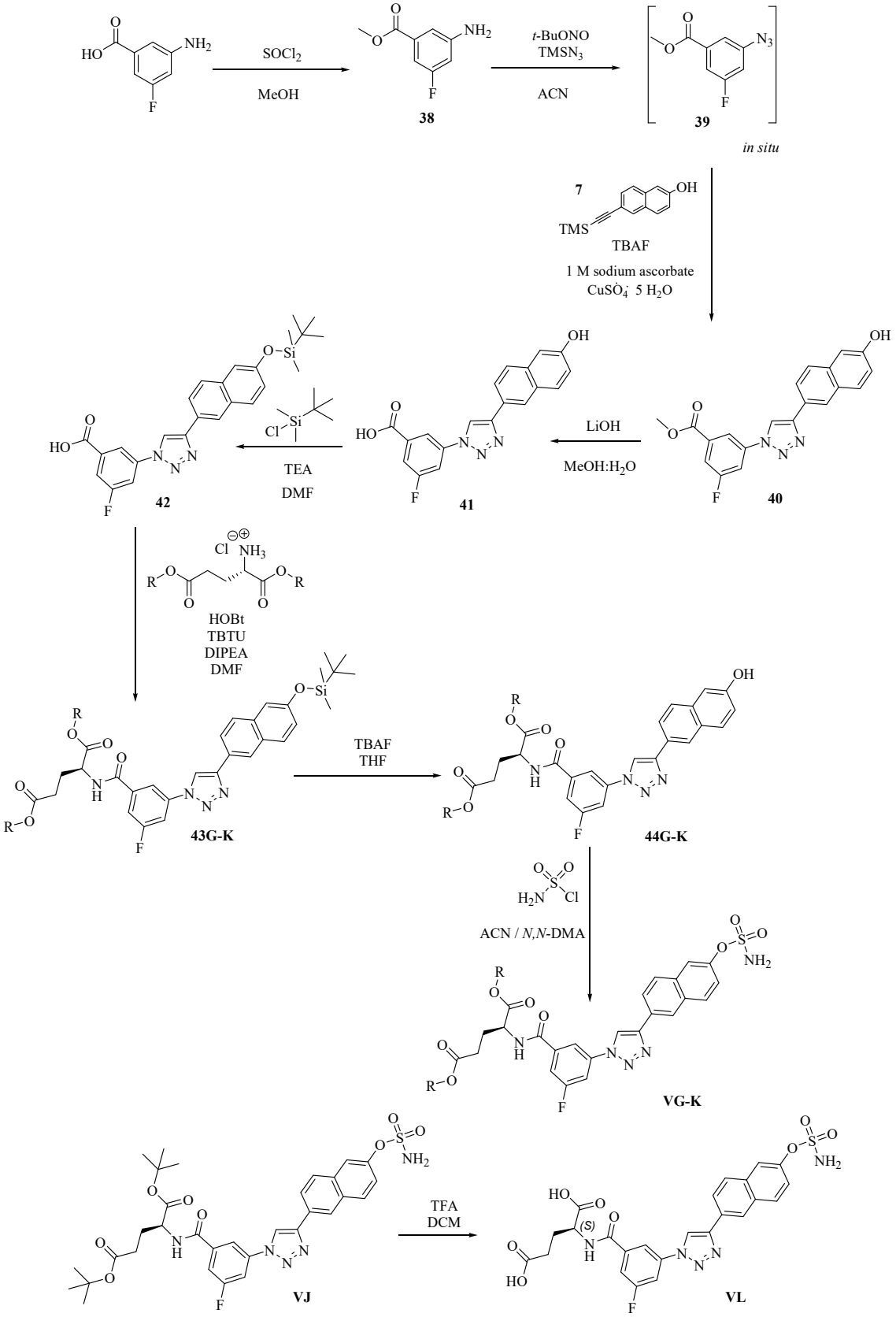

Scheme 6. Synthetic pathway for compounds **VG-L** (R = Me, Et, ^{i}Pr, ^{t}Bu, Bn).

Biological evaluation

In the next step of our investigation, all of the synthesized compounds were biologically evaluated in enzymatic and cellular experiments using radiolabeled estrone sulfate ([^{3}H]E1S) as a substrate. The collected data were summarized in **Table 3** and **Table 4**. Initially, to verify their STS inhibitory potency, a screening assay using STS enzyme isolated from the human placenta was performed for the first series of synthesized derivatives **I-IVA-B** at 10 μM concentration. Because intermediates **19**, **25**, and **30** also contained sulfamate pharmacophore in the chemical structure we decided to include them in the examined set of compounds. The highest STS inhibitory potency with remaining STS activities of 4.35% and 8.17% was demonstrated by the coumarin derivative **IIA** and the derivative **30** based on flavone core, respectively (**Table 3**). Importantly, their STS inhibitory potency were found to be comparable with activity determined for the reference STS inhibitor *Irosustat* **1** (with remaining STS activity of 6.31%). Unexpectedly, tyramine derivatives **IIIA** and **IIIB** were found to be inactive in enzymatic assay. According to the collected data, it was not possible to determine which form of the glutamic acid residue is the most beneficial for the highest STS inhibitory activity of the compounds. For the next step of biological evaluation, we selected compounds **IB**, **IIA**, **IIB**, **25**, and **30**, for which the remaining STS activity, as determined in enzymatic assay, was below 40%. The experiment with JEG-3 cells revealed that the triazole-containing derivative **IB** exhibits the highest STS inhibitory activity with the IC_{50} value of 1436 nM. Unfortunately, the activity of the compound **IB** occurred to be significantly lower than the STS inhibitory potency of *Irosustat* **1** (IC_{50} = 2.7 nM). Despite the high activity in enzymatic assay, derivatives **IIB** and **30** were inactive in cellular assay indicating that these compounds may show limitations with penetration into the cells or are metabolically unstable after uptake.

Table 3. STS inhibitory activity of the compounds **I-IVA-B** in enzymatic and cellular assay.

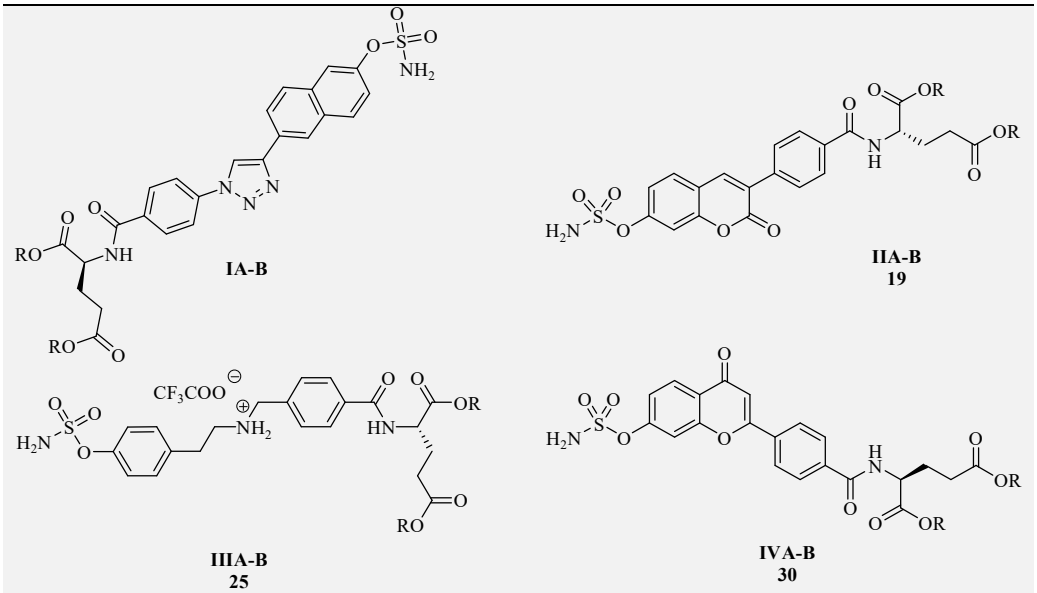

No.	R	Remaining STS activity in enzymatic assay [%]	IC_{50} determined in cellular assay[nM]
IA	Me	79.28 ± 4.81	-
IB	H	25.28 ± 2.78	**1436 ± 244**
IIA	Me	4.35 ± 0.20	2655 ± 671
IIB	H	30.36 ± 0.83	>5000

19	^{t}Bu	41.75 ± 2.53	-
IIIA	Me	100.00 ± 3.62	-
IIIB	H	100.00 ± 7.42	-
25	^{t}Bu	21.84 ± 0.51	4336 ± 649
IVA	Me	44.84 ± 2.00	-
IVB	H	74.09 ± 3.20	-
30	^{t}Bu	8.17 ± 1.03	>20000
Irosustat **1**	-	6.31 ± 1.18	2.7 ± 0.2

Due to the moderate STS inhibitory activity of the first series of compounds, we decided to select the most active inhibitor **IB** and modify its structure to obtain a larger series of STS inhibitors based on triazole core. In the second series of compounds **VA-L**, we introduced a fluorine atom in *meta* position of the terminal phenyl ring of compound **IB**. We supposed that this modification would enhance the STS inhibitory potency as we had seen previously in other series of STS inhibitors developed in our research group [10, 17, 18]. Moreover, we decided to evaluate the influence of the glutamic acid residue position in the terminal phenyl ring. Furthermore, different alcohols were utilized in the creation of ester groups of glutamic acid. Following the approach of the first series of inhibitors, we evaluated the STS inhibitory activity of the newly synthesized compounds **VA-L** in enzymatic and cellular experiments. The initial assessment of the compounds **VA-L** in the enzymatic assay was performed using three different concentrations of inhibitors (10 μM, 1 μM, and 0.1 μM). The collected data revealed (**Table 4**) that all of the synthesized compounds show promising STS inhibitory activity. In general, derivatives with the glutamic acid residue located at *meta* position of the terminal phenyl ring (relative to triazole unit) demonstrated higher STS inhibitory potency than their *para*-substituted analogs. Within the series of compounds, the derivative **VK** containing a benzyl ester exhibited the highest STS inhibitory activity with a remaining STS activity value of 20.52% at 0.1 μM inhibitor concentration. This result was consistent with the molecular modeling data, which indicated that derivative **VK** demonstrated the highest theoretical affinity to the STS active site. The STS inhibitory activity of the compound **VK** occurred to be slightly lower than the activity of *Irosustat* **1**, for which the remaining STS activity value was 6.46% at the same concentration. The evaluation of anti-STS activity with JEG-3 cells indicated that the introduction of a fluorine atom was found to be beneficial for STS inhibitory potency of the compounds. Almost all of the newly synthesized analogs showed higher STS inhibitory activity than parental compound **IB** (the only exception was compound **VG** with the IC_{50} value of 3035 nM). It may be explained by the electron-withdrawing effect of the fluorine atom, which cases higher reactivity of sulfamate group in the reaction with catalytic fGly75 residue in the enzyme's active site. As found in the enzymatic assay, the derivative **VK** turned out be the most active also in the experiments with JEG-3 cells. The IC_{50} value of 22 nM determined for compound **VK** was slightly higher than that of *Irosustat* **1** (2.7 nM). However, more derivatives with the glutamic acid residue substituted at *meta* position demonstrated high nanomolar STS inhibitory activity confirming that this location is beneficial for the potency of the compounds. Unfortunately, due to the low solubility of compounds **VA**, **VD**, and **VE**, determination of their IC_{50} values was not possible.

Table 4. STS inhibitory effect of the newly synthesized compounds **VA-K** in enzyme assay and cellular assay using JEG-3 cells.

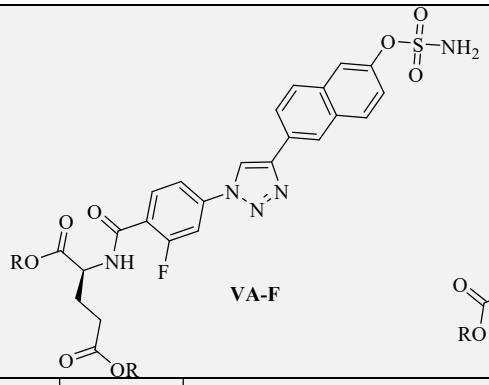

VA-F

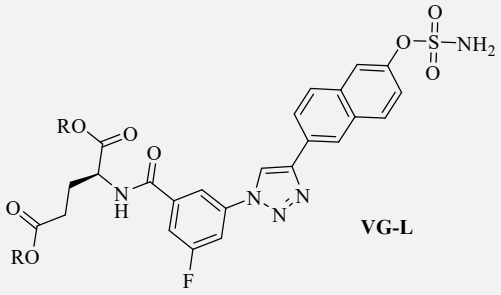

VG-L

No	R	Remaining STS activity in enzymatic assay [%]			IC_{50} determined in cellular assay [nM]
		10 µM	**1 µM**	**0.1 µM**	
VA	Me	24.86 ± 4.26	39.91 ± 1.23	100.00 ± 4.49	-
VB	Et	26.3 ± 0.89	41.50 ± 5.40	100.00 ± 2.81	1259 ± 209.8
VC	^{i}Pr	38.28 ± 4.22	68.24 ± 3.66	100.00 ± 4.23	1393 ± 209.4
VD	^{t}Bu	53.89 ± 9.12	81.39 ± 3.39	84.32 ± 5.33	-
VE	Bn	30.99 ± 3.15	54.51 ± 5.63	76.98 ± 9.56	-
VF	H	16.95 ± 7.46	65.22 ± 3.39	92.44 ± 9.12	689 ± 302.6
VG	Me	17.08 ± 19.91	41.9 ± 20.61	99.64 ± 6.47	3035 ± 685
VH	Et	15.18 ± 1.50	33.73 ± 0.86	90.15 ± 5.70	362 ±82.3
VI	^{i}Pr	13.59 ± 2.50	17.70 ± 1.36	66.70 ± 4.13	179 ± 42.2
VJ	^{t}Bu	10.63 ± 1.50	15.46 ± 0.54	39.72 ± 2.25	393 ± 292
VK	Bn	**12.97 ± 4.57**	**17.58 ± 2.60**	**20.52 ± 2.08**	**22** ± 3.7
VL	H	16.31 ± 0.88	52.99 ± 5.20	93.3 ± 8.06	600 ± 238
Irosustat **1**	-	6.31 ± 1.18	5.11 ± 1.07	6.46 ± 1.35	2.7 ± 0.2

In the final step of biological studies, we investigated if the most active STS inhibitor **VK** could be potentially transported into the cancer cell by receptors involved in the folate uptake pathway. For this purpose, we incubated compound **VK** with JEG-3 cells at the concentration of 1µM without or in the presence of FA at 1 mM concentration. Theoretically, the addition of FA at a high concentration should saturate folate transporters (*e.g.*, FRα) leading to the loss of activity of compounds that are actively transported through this mechanism. Unfortunately, the remaining STS activity after incubation with compound **VK** in the presence of FA occurred to be comparable with the remaining STS activity measured for compound **VK** without the addition of FA, 44% and 42%, respectively. This observation does not rule out that compound **VK** may be transported by the receptors involved in the FA transport, however, the results suggest that there is another mechanism ensuring the uptake into cells. Alternatively, high passive diffusion through the cellular membrane of the compound **VK** may also be possible.

Conclusions

In the present work, we have described convenient methods for the synthesis of different types of novel non-steroidal STS inhibitors containing an additional glutamic acid residue in the structure. The molecular modeling studies indicated that designed derivatives of coumarin, tyramine, triazole, and flavone can bind to the STS active site as well as to the FRα binding

site, at least theoretically. The biological activity of synthesized compounds was evaluated under a two-step procedure including enzymatic assay as a screening for the most promising agents and cellular studies using JEG-3 cells. Among the first series of synthesized compounds, derivatives **IB** containing triazole ring occurred to be the most active in the cellular experiment with an IC_{50} value of 1.436 μM. Next, compound **IB** was selected as the most promising STS inhibitor and its structure was modified by the addition of a fluorine atom in *meta* position of the terminal phenyl ring, relative to the triazole unit. Furthermore, we decided to evaluate the influence of the glutamic acid residue position, as well as to use different alcohols in the creation of ester groups of glutamic acid. In general, the obtained series of compound **VA-L** demonstrated higher STS inhibitory activity than parental compound **IB** proving that the introduction of a fluorine atom was beneficial for STS inhibitory potency. It may be explained by the electron-withdrawing effect of the fluorine atom, which cases higher reactivity of sulfamate group in the reaction with the catalytic fGly75 of STS. Derivative **VK** occurred to be the most active, in both, enzymatic assays and experiments with JEG-3 cells. The IC_{50} value of 22 nM determined in cellular studies for compound **VK** was close to the IC_{50} value determined for *Irosustat* **1** (2.7 nM). During the course of our studies, we observed that derivatives with the glutamic acid residue substituted at *meta* position relative to the triazole ring demonstrated high nanomolar STS inhibitory activity, further confirming that this location is beneficial for the potency of compounds. Unfortunately, the experiment with the folate receptors saturation did not confirm that the compound **VK** is actively transported into the cell mainly by the receptors involved in the FA uptake. Additional studies are necessary for the determination of the transport mechanism for this compound.

Experimental

Chemistry

Substrates for synthesis: 6-bromo-2-naphthol, trimethylsilylacetylene, palladium(II) chloride, triphenylphosphine, copper(I) iodide, TEA, the appropriate aniline derivatives, *t*-BuONO, $TMSN_3$, 1 M solution of TBAF in THF, sodium ascorbate, copper(II) sulfate pentahydrate, *para*-aminobenzoic acid, thionyl chloride, lithium hydroxide, hydroxybenzotriazole, sulphamoyl chloride, 4-(carboxymethyl)benzoic acid, 2,4-dihydroxybenzaldehyde, 4-(2-aminoethyl)phenol, 4-formylbenzoic acid, 1-(2-hydroxy-4-methoxyphenyl)ethanone, 4-amino-2-fluorobenzoic acid, 3-amino-5-fluorobenzoic acid, TBTU, DIPEA, TFA, Boc_2O, potassium carbonate, sodium cyanoborohydride, *tert*-butyldimethylsilyl chloride were commercially available from Sigma-Aldrich, Chemat or Fluorochem. Solvents: ACN, DCM, methanol (MeOH), acetone, *N,N*-DMA, *N,N*-dimethylformamide (*N,N*-DMF) were dried and distilled using standard procedures. Melting points (uncorrected) were determined with a Stuart Scientific SMP30 apparatus. ^1H and ^{13}C NMR spectra were recorded on a Bruker Avance III HD 400 MHz spectrometer and Varian Inova 500 MHz spectrometer. Chemical shifts δ are reported in parts per million relative to the residual solvent peak ($CDCl_3$ = 7.26 ppm for ^1H, 77.0 ppm for ^{13}C, DMSO-d_6 2.49 ppm for ^1H, and 39.5 ppm for ^{13}C). Coupling constants are given in Hertz. Mass spectra were recorded on Agilent 6540 Accurate Mass Q-TOF LC/MS System and TripleTOF 5600+ (SCIEX, Framingham, MA, USA). Preparative thin-layer chromatography (TLC) was carried out with Polygram SIL G/UV254, silica gel (Macherey-Nagel GmbH & Co. KG, Düren, Germany). Column chromatography was performed using silica gel (230-400 mesh, Merck). Flash chromatography was carried out using Büchi FlashPure cartridges (10 μm irregular silica gel) on a Büchi Pure chromatography system with an integrated UV and ELSD detector. The procedures for the synthesis of all intermediates and final compounds are described in detail in *Supporting information*.

Molecular modeling

Ligands preparation

The 3D structure of ligands **IA-B, IIA-B, IIIA-B, IVA-B, VA-L,** and reference compounds (*Irosustat* **1** and FA) were prepared with the Portable HyperChem 8.0.7 Release (Hypercube, Inc., Gainesville, FL, USA). Before docking calculations, the structure of each ligand was optimized using an MM+ force field and the Polak–Ribière conjugate gradient algorithm (terminating at a gradient of 0.05 kcal mol^{-1} $Å^{-1}$).

Molecular targets preparation

The X-ray structures of the STS and FRα used for molecular modeling studies were taken from the Protein Databank (Protein Data Bank accession codes: 1P49 and 4LRH respectively). After standard preparation procedures (including the removal of water molecules and other ligands as well as the addition of hydrogen atoms and Gasteiger charges to each atom) docking analysis was carried out. In the case of STS, the catalytic amino acid fGly75 was converted to the gem-diol form using the Protein Preparation Wizard module, delivered with Maestro (Schrödinger, LLC, New York, NY, USA).

Molecular docking

Docking studies were carried out using Autodock Vina 1.1.2 software (The Molecular Graphic Laboratory, The Scripps Research Institute, La Jolla, CA, USA) [20] with exhaustiveness, num_modes, and energy_range parameters set as 8, 30, and 10, respectively. For the docking studies the corresponding grid box parameters were used:

- STS: a grid box size of 30 Å x 30 Å x 30 Å centered on the Cβ off Gly75 amino acid residue (x = 72.135, y = -1.720, z = 28.464);
- FRα: a grid box size of 30 Å x 30 Å x 30 Å centered on Cα of Trp135 amino acid residue (x = 6.875, y = 17.597, z = 1.904).

Graphic visualizations of the 3D model were generated using VMD 1.9 software (University of Illinois at Urbana – Champaign, Urbana, IL, USA). Identification of the ligand-protein interactions was performed using Discovery Studio Visualiser v20. 1. 0. 19295 (BIOVIA, Dassault Systémes, San Diego, CA, USA).

Biological assays

The inhibitory potency of the synthesized compounds was examined in two ways, including an enzymatic assay and the radioisotope cellular test. The enzymatic assay was performed using the STS enzyme extracted from the human placenta and purified to homogeneity following a multi-step chromatography protocol as previously described [21] and radiolabeled [^{3}H]E1S as a substrate. The radioisotope cellular assay was performed using the JEG-3 cell line in the presence of radiolabeled [^{3}H]E1S. Radiolabelled [^{3}H]E1S for enzyme and cellular assays was purchased from PerkinElmer.

In vitro enzymatic assay

Evaluation of the inhibitory property of each compound was performed in the reaction mixture containing 20 mM Tris-HCl, pH 7.4, [^{3}H]E1S (4×10^4 Bq, 3 nM), 10, 1 or 0.1 μM inhibitor, and 5 U of the purified enzyme (1 U is the amount of enzyme that hydrolyzes 100 μM *p*-nitrophenyl sulfate at 37°C in 1 h). The total volume of the reaction mixture was 100 μL. The experiments were performed for 1 h at 37 °C. After incubation, the reaction mixture

(90 µL) was collected from each well, and the product formed by STS hydrolysis was extracted with toluene (0.5 mL). STS activity was measured using a MicroBeta radioluminometer (PerkinElmer). Enzymatic assays were carried out in triplicate.

***In vitro* cellular assay**

The evaluation of the inhibitory effect of each compound on choriocarcinoma cell line JEG-3 was performed using a method that we previously described with some modifications [17]. JEG-3 cells were maintained in Dulbecco's modified Eagle medium supplemented with 10% fetal bovine serum and cultured in the above medium until 80% confluence. For the measurement of STS inhibitory potency, cells were seeded in 96-well microplates (Nest Biotechnology) at a density of 2×10^4 cells/well (the number of cells was determined using a Scepter 3.0 Handheld Automated Cell Counter). Incubation of the cells was performed for 20 h at 37°C in a 5% CO_2 humidified incubator in a serum-free medium (0.1 mL) with the addition of [^{3}H]E1S (4×10^4 Bq, 3 nM) in the absence or presence of the inhibitor at an appropriate concentration: 0.1, 1, or 10 µM. After incubation, the medium (0.09 mL) was collected from each well, and the product formed by STS hydrolysis was extracted with toluene (0.5 mL). STS activity was measured using a MicroBeta radioluminometer (PerkinElmer). Assays with JEG-3 cells were carried out in triplicate. In addition, folate competition experiments were conducted by incubation of the cells in the presence of 1 mM of FA. IC_{50} values of selected compounds were calculated with the use of GraphPad software.

Abbreviations

[^{3}H]E1S	-	[^{3}H] estrone sulfate
ACN	-	acetonitrile
BOC	-	*tert*-butoxycarbonyl protective group
Boc_2O	-	di-*tert*-butyl dicarbonate
DCM	-	dichloromethane
DIPEA	-	*N*,*N*-diisopropylethylamine
ER	-	estrogen receptor
FA	-	folic acid
FRα	-	folate receptor α
HOBt	-	1-hydroxybenzotriazole
MeOH	-	methanol
N,*N*-DMA	-	*N*,*N*-dimethylacetamide
N,*N*-DMF	-	*N*,*N*-dimethylformamide
PDB	-	Protein Data Bank
PY•HCl	-	pyridine hydrochloride
STS	-	steroid sulfatase
TBAF	-	tetra-*n*-butylammonium fluoride
TBDMS	-	*tert*-butyldimethylsilyl
TBTU	-	2-(1*H*-benzotriazole-1-yl)-1,1,3,3-tetramethylaminium tetrafluoroborate
t-BuONO	-	tert-butyl nitrite
TEA	-	triethylamine
TFA	-	trifluoroacetic acid
THF	-	tetrahydrofurane
$TMSN_3$	-	trimethylsilyl azide
TLC	-	thin layer chromatography

CRediT authorship contribution statement

Olga Ciupak: Investigation, Methodology, Writing – original draft, Data curation, Funding acquisition. **Sebastian Demkowicz**: Supervision, Writing – review and editing. **Janusz Rachon**: Writing – review and editing. **Karol Biernacki**: Investigation, Writing – review and editing. **Paweł Czubak**: Investigation, Methodology. **Aleksandra Martyna**: Investigation, Methodology. **Maciej Masłyk**: Conceptualization, Validation. **Konrad Kubiński**: Conceptualization, Validation, Writing – review and editing. **Magdalena Datta**: Investigation, Writing – review and editing. **Janusz Rak**: Writing – review and editing. **Mateusz Daśko**: Conceptualization, Investigation, Methodology, Validation, Data curation, Writing – original draft, Formal analysis.

Declaration of competing interest

The authors declare that they have no known competing financial interests or personal relationships that could have appeared to influence the work reported in this paper.

Acknowledgements

This work was supported by the National Science Centre (Poland) (PRELUDIUM grant no. UMO-2021/41/N/NZ7/01851).

Appendix A. Supplementary data

Supplementary data to this article can be found online.

Data availability

Data will be made available on request.

References

[1] Clusan, L.; Ferrière, F.; Flouriot, G.; Pakdel, F.; A basic review on estrogen receptor signaling pathways in breast cancer. *Internat. J. Mol. Sci.* **2023**, 24, 6834, doi: 10.3390/ijms24076834.

[2] Schiewer, M.; Knudsen, K.; Linking DNA damage and hormone signaling pathways in cancer. *Trends Endocrinol. Metab.* **2016**, 27, 216-225, doi: 10.1016/j.tem.2016.02.004.

[3] Daśko, M.; Demkowicz, S.; Biernacki, K.; Ciupak, O.; Kozak, W.; Masłyk, M.; Rachoń, J.; Recent progress in the development of steroid sulfatase inhibitors – examples of the novel and most promising compounds from the last decade. *J. Enzyme Inhibit. Med. Chem.* **2020**, *35*, 1163-1184, doi: 10.1080/14756366.2020.1758692.

[4] Secky, L.; Svoboda, M.; Klameth, L.; Bajna, E.; Hamilton, G.; Zeillinger, R.; Jäger, W.; Thalhammer, T.; The sulfatase pathway for estrogen formation: targets for the treatment and diagnosis of hormone-associated tumors. *J. Drug Deliv.* **2013**, 1-13, doi: 10.1155/2013/957605.

[5] Palmieri, C.; Szydlo, R.; Miller, M.; Barker, L.; Patel, N.H.; Sasano, H.; Barwick, T.; Tam, H.; Hadjiminas, D.; Lee, J.; Shaaban, A.; Nicholas, H.; Coombes, R.C.; Kenny, L.M.; IPET study: an FLT-PET window study to assess the activity of the steroid sulfatase inhibitor irosustat in early breast cancer. *Breast Cancer Res. Treat.* **2017**, 166, 527-539, doi: 10.1007/s10549-017-4427-x.

[6] Potter, B.; Sulfation pathways: steroid sulphatase inhibition via aryl sulphamates: clinical progress, mechanism and future prospects. *J. Mol. Endocrinol.* **2018** 61, T233-T252, doi: 10.1530/JME-18-0045.

[7] Daśko, M.; Demkowicz, S.; Biernacki, K.; Harrous, A.; Rachoń, J.; Kozak, W.; Martyna, A.; Masłyk, M.; Kubiński, K.; Boguszewska-Czubara, A.; Novel steroid sulfatase inhibitors

based on N-thiophosphorylated 3-(4-aminophenyl)-coumarin-7-O-sulfamates. *Drug Dev. Res.* **2019**, 80, 857-866, doi: 10.1002/ddr.21569.
[8] Kozak, W.; Daśko, M.; Masłyk, M.; Kubiński, K.; Rachoń, J.; Demkowicz, S.; Steroid Sulfatase Inhibitors Based on Phosphate and Thiophosphate Flavone Analogs. *Dryg Dev. Res.* **2015**, 76, 450-462, doi: 10.1002/ddr.21281.
[9] Daśko, M.; Rachoń, J.; Masłyk, M.; Kubiński, K.; Demkowicz, S.; Synthesis and biological evaluation of N-acylated tyramine sulfamates containing C-F bonds as steroid sulfatase inhibitors. *Chem. Biol. Drug Des.* **2017**, 90, 156-161, doi: 10.1111/cbdd.12931.
[10] Biernacki, K.; Ciupak, O.; Daśko, M.; Rachon, J.; Kozak, W.; Rak, J.; Kubiński, K.; Masłyk, M.; Martyna, A.; Śliwka-Kaszyńska, M.; Wietrzyk, J.; Świtalska, M.; Nocentini, A.; Supuran, C. T.; Demkowicz, S.; Development of Sulfamoylated 4-(1-Phenyl-1H-1,2,3-triazol-4-yl)phenol Derivatives as Potent Steroid Sulfatase Inhibitors for Efficient Treatment of Breast Cancer. *J. Med. Chem.* **2022**, 65, 5044-5056, doi: 10.1021/acs.jmedchem.1c02220.
[11] Ali, I.; Wani, W.A.; Haque, A.; Saleem, K.; Glutamic acid and its derivatives: Candidates for rational design of anticancer drugs, *Future Med. Chem.* **2013**, 5, 961-978, doi: 10.4155/fmc.13.62.
[12] Vale, N.; Ferreira, A.; Matos, J.; Fresco, P.; Gouveia, M.J.; Amino acids in the development of prodrugs. *Molecules* **2018**, 23, 2318, doi: 10.3390/molecules23092318.
[13] Kyoung, M.K.; Oh, Y.M.; Park, K.-S.; Chong, Y. A novel prodrug of quercetin, 3-N,N-dimethyl carbamoyl quercetin (DCQ), with improved stability against hydrolysis in cell culture medium. *Bull. Korean Chem. Soc.* **2009**, 30, 2114–2116, doi: 10.5012/bkcs.2009.30.9.2114.
[14] Chen, Ch.; Ke, J.; Zhou, X.E.; Yi, W.; Brunelle, J.S.; Li, J.; Yong, E.L.; Xu, H.E.; Melcher, K.; Structural basis for molecular recognition of folic acid by folate receptors. *Nature*, **2013**, 500, 486-489, doi: 10.1038/nature12327.
[15] Elnakat, H.; Distribution, functionality and gene regulation of folate receptor isoforms: implications in targeted therapy. *Adv. Drug Deliv. Rev.* **2004**, 56, 1067, doi: 10.1016/j.addr.2004.01.001.
[16] Srinivasarao, M.; Galliford, C.V.; Low, P.S.; Principles in the design of ligand-targeted cancer therapeutics and imaging agents. *Nat. Rev.* **2015**, 14, 203-219, doi: 10.1038/nrd4519.
[17] Ciupak, O.; Daśko, M.; Biernacki, K.; Rachoń, J.; Masłyk, M.; Kubiński, K.; Martyna, A.; Demkowicz, S.; New potent steroid sulphatase inhibitors based on 6-(1-phenyl-1H-1,2,3-triazol-4-yl)naphthalen-2-yl sulphamate derivatives. *J. Enzyme Inhibit. Med. Chem.* **2021**, 36, 239-248, doi: 10.1080/14756366.2020.1858820.
[18] Daśko, M.; Demkowicz, S.; Rachoń, J.; Biernacki, K.; Aszyk, J.; Kozak, W.; Masłyk, M.; Kubiński, K.; New potent STS inhibitors based on fluorinated 4-(1-phenyl-1H-[1,2,3]triazol-4-yl)-phenyl sulfamates. *J. Asian Nat. Prod. Res.* **2019**, 22, 1037-1044, doi: 0.1080/10286020.2019.1680642.
[19] Kobzar, O.L.; Tatarchuk, A.V.; Mrug, G.P.; Bondarenko, S.P.; Demydchuk, B.A.; Frasinyuk, M.S.; Vovk, A.I.; Carboxylated chalcones and related flavonoids as inhibitors of xanthine oxidase, *Med. Chem. Res* **2023**, 32, 1804–1815, doi: 10.1007/s00044-023-03109-8.
[20] Trott, O.; Olson, A. J.; AutoDock Vina: Improving the speed and accuracy of docking with a new scoring function, efficient optimization, and multithreading. *J. Comput. Chem.* **2010**, 31, 455-461, doi: 10.1002/jcc.21334.
[21] Hernandez-Guzman, F. G.; Higashiyama, T.; Osawa, Y. Ghosh, D.; Purification, characterization and crystallization of human placental estrone/dehydroepiandrosterone sulfatase, a membrane-bound enzyme of the endoplasmic reticulum. *J. Steroid Biochem. Mol. Biol.* **2001**, 78, 441-450, doi: 10.1016/s0960-0760(01)00119-4.